



Supplement of

SYSU TWSA v1.0: global high-resolution terrestrial water storage anomalies via satellite gravimetry

Yuhao Xiong et al.

Correspondence to: Wei Feng (fengwei@sysu.edu.cn)

The copyright of individual parts of the supplement might differ from the article licence.

S1. Comparison with GLDAS CLSM DA V2.2

Figure S1 compares GLDAS CLSM DA v2.2 with GRACE/GFO in 288 global level-3 basins. Table S1 shows that, although GLDAS CLSM DA v2.2 and GLWS are both derived through EnKF assimilation, GLDAS CLSM DA v2.2 exhibits close agreement with GRACE/GFO across multiple metrics (RMSE=2.61 cm, NSE=0.43, CC=0.75, and $R^2=0.66$), whereas the agreement is weak for GLWS (RMSE=3.4 cm, NSE=0.14, CC=0.68, and $R^2=0.45$). Nevertheless, the SYSU product (RMSE=2.24 cm, NSE=0.71, CC=0.90, and $R^2=0.92$) and the Gou's product (RMSE=1.87 cm, NSE=0.68, CC=0.88, and $R^2=0.83$) show closer agreement with GRACE/GFO than GLDAS CLSM DA v2.2 in the 288 basins. Notably, GLDAS CLSM DA v2.2 shows degraded performance in arid regions and in glacierized areas (e.g., Alaska), likely because the CLSM framework lacks an explicit module for mountain-glacier processes.

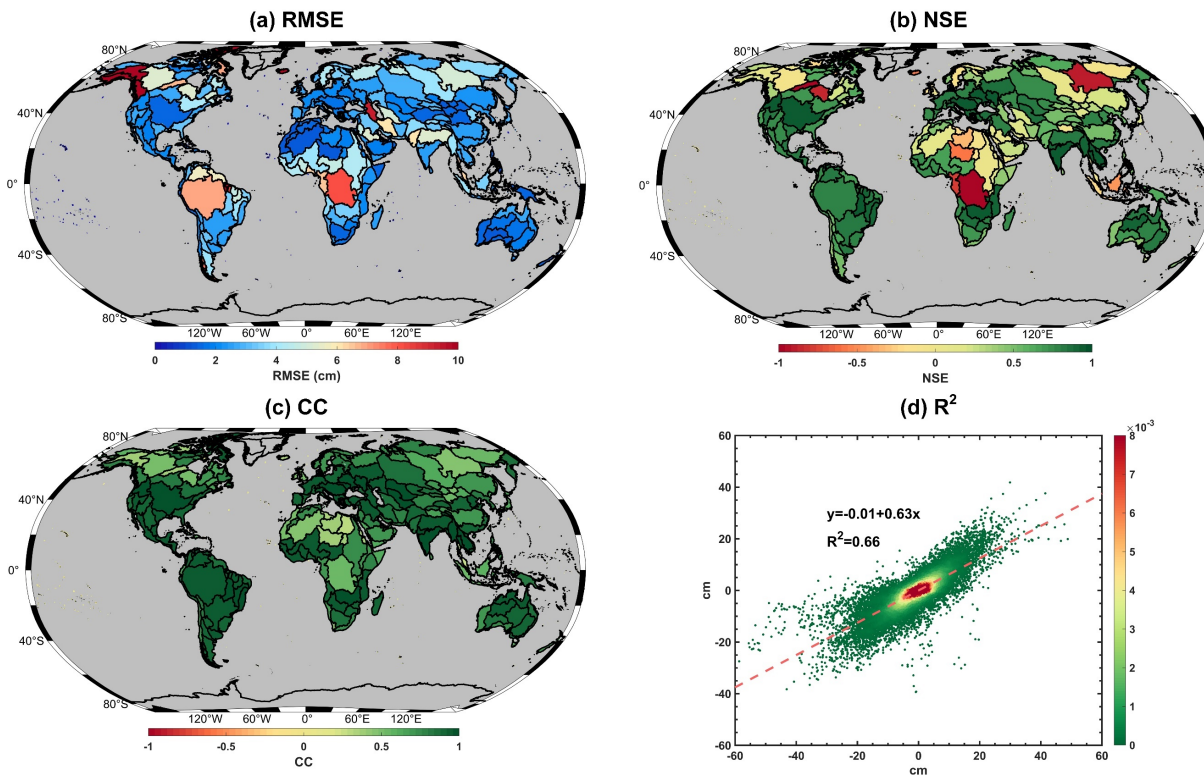


Figure S1: Basin-wise comparison of GLDAS CLSM DA v2.2 product with GRACE/GFO observations: (a) RMSE, (b) NSE, (c) CC, and (d) scatter plot validation (R^2 indicates the goodness of fit).

S2. Sensitivity to WGHM-derived spatial priors

To examine the sensitivity of SYSU to WGHM-derived spatial priors, we reconstructed the product using two WGHM configurations: one neglecting direct human impacts (WGHM-NHI) and one including direct human impacts (WGHM-HI). The comparison shows that WGHM-NHI largely misses negative trends in several regions affected by intensive groundwater abstraction, whereas WGHM-HI better represents these human-induced depletion signals. After joint inversion, both downscaling results are constrained by GRACE/GFO observations, but regional differences remain in groundwater-dominated areas. In particular, the downscaling result using WGHM-HI priors better preserves negative trends in representative groundwater depletion regions, such as northwestern India, the North China Plain, and other intensively managed aquifer systems.

Despite this sensitivity to WGHM spatial priors, the joint-inversion framework still improves the basin-scale consistency between WGHM-NHI and GRACE/GFO. As shown in Fig. S3, the original WGHM-NHI outputs show relatively large RMSE and lower NSE or CC in several basins. After joint inversion using WGHM-NHI-derived spatial priors, the agreement with GRACE/GFO improves substantially across most basins. This indicates that the framework can effectively combine the high-resolution spatial information provided by WGHM with the reliable large-scale temporal variability observed by GRACE/GFO. However, because the spatial allocation of signals is still controlled by the WGHM-derived basis functions, groundwater-dominated and heavily managed regions remain sensitive to the quality of the underlying model spatial priors.

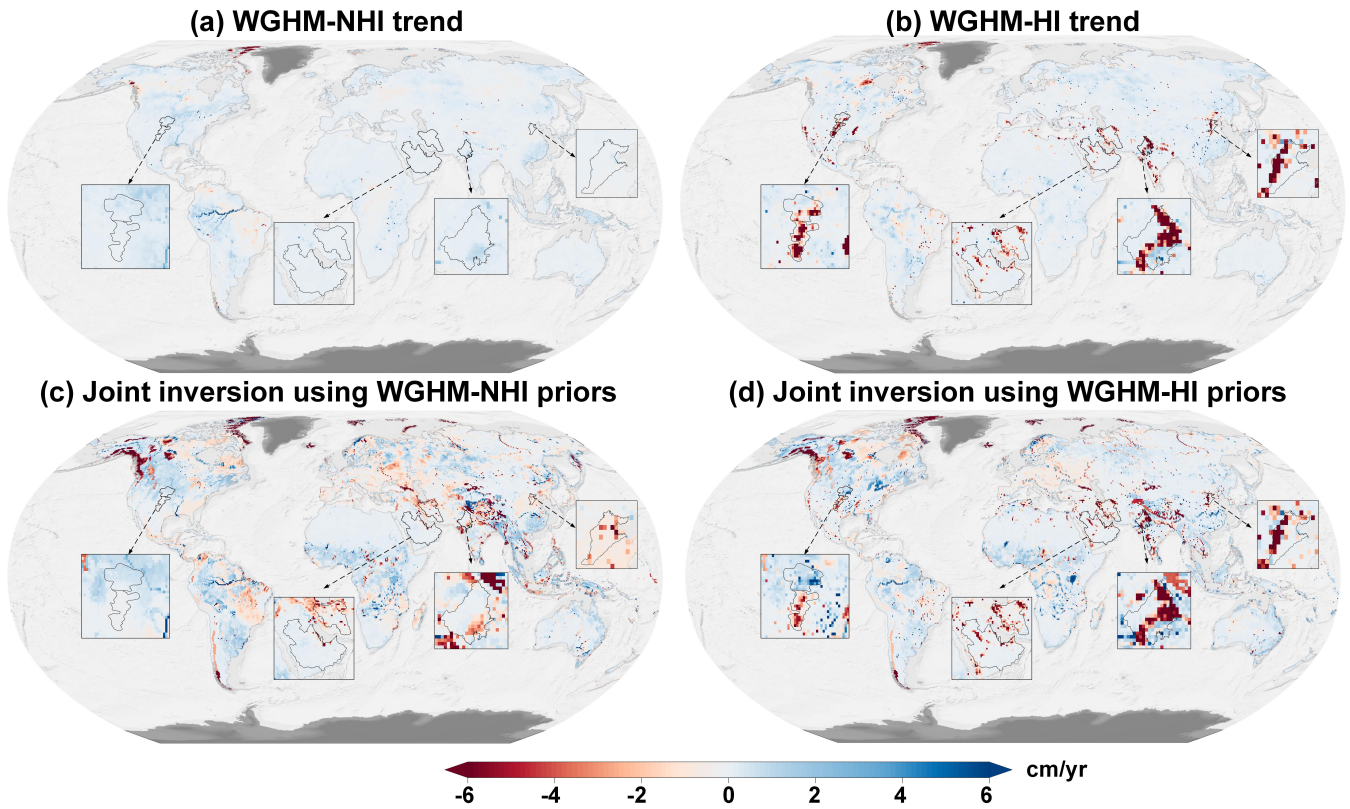
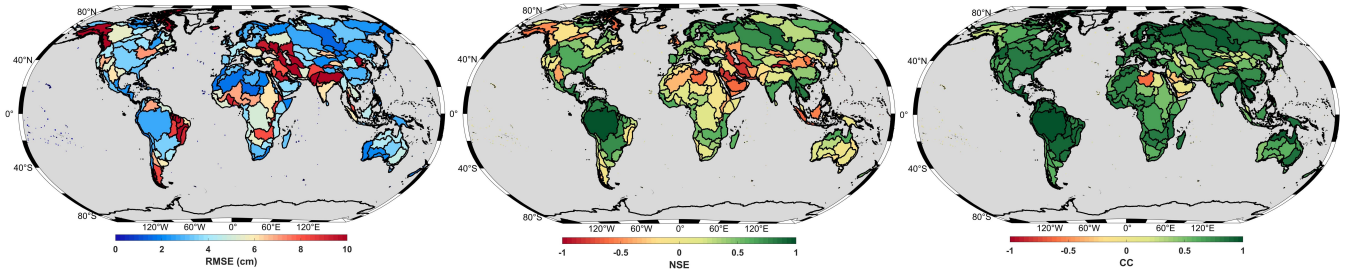


Figure S2: Sensitivity of downscaling TWSA trends to the representation of direct human impacts in WGHM. (a) TWSA trend from WGHM outputs neglecting direct human impacts (WGHM-NHI). (b) TWSA trend from WGHM outputs including direct human impacts (WGHM-HI). (c) Joint-inversion downscaling results using WGHM-NHI-derived spatial priors. (d) Joint-inversion downscaling results using WGHM-HI-derived spatial priors. Insets highlight representative regions with strong human-induced groundwater depletion. Units are cm/yr.

(a) Before joint inversion: WGHM-NHI vs GRACE/GFO



(b) After joint inversion: downscaled TWSA vs GRACE/GFO

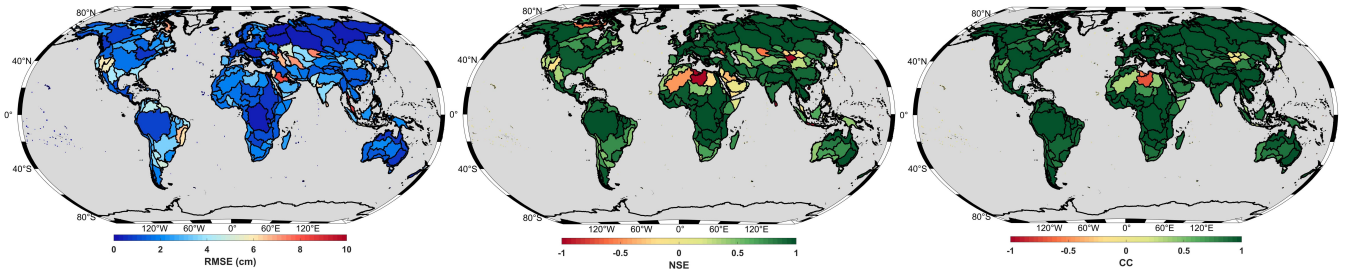


Figure S3: Basin-scale consistency with GRACE/GFO before and after joint inversion using WGHM-NHI spatial priors. The first row shows the comparison between WGHM outputs neglecting direct human impacts (WGHM-NHI) and GRACE/GFO in terms of RMSE, NSE, and CC. The second row shows the corresponding comparison after joint-inversion downscaling result using WGHM-NHI-derived spatial priors, including RMSE, NSE, and CC. The results show that joint inversion substantially improves basin-scale consistency with GRACE/GFO, even when the spatial priors are derived from WGHM outputs that neglect direct human impacts. This indicates that the framework effectively combines high-resolution model-derived spatial information with large-scale temporal constraints from GRACE/GFO. RMSE is given in cm.

Table S1. Evaluation of different products in 288 basins. Metrics include the median values of RMSE (in cm), NSE, CC, and R². For each row, the best-performing value is shown in bold, and the second-best is underlined.

Product type	RMSE	NSE	CC	R ²
SYSU	<u>2.24</u>	0.71	0.90	0.92
Gou and Soja (2024)	1.87	<u>0.68</u>	<u>0.88</u>	<u>0.83</u>
GLDAS CLSM DA v2.2	2.61	0.43	0.75	0.66
GLWS	3.40	0.14	0.68	0.45
WGHM	3.27	0.14	0.65	0.26